Heliyon 10 (2024) e38593

Contents lists available at ScienceDirect

Heliyon

journal homepage: www.cell.com/heliyon

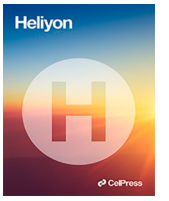

Research article

Benzothiazole-quinoline based probe for simultaneous colorimetric detection of CN- and Cu2+ ions, with fluorescence sensing for Cu2+: Mechanistic insights and practical applications in environmental monitoring and cellular analysis

P.S. Umabharathi [a], S. Karpagam [a,*], Tiasha Dasgupta [b], Ramasamy Tamizhselvi [b]

[a] Department of Chemistry, School of Advanced Sciences, Vellore Institute of Technology, Vellore, 14, Tamil Nadu, India
[b] School of Bio Science and Technology, Vellore Institute of Technology, Vellore, 14, Tamilnadu, India

ARTICLE INFO

Keywords:
Multifunctional
Cyanide ion
Copper ion
Colorimetric
Azomethine
Sensing tool
DFT

ABSTRACT

The development and synthesis of notably targeted and colorimetric sensor based on an azomethine compound for the distinct recognition of Cu^{2+} and CN^{-} ion individually in an aqueous dimethyl formamide solution is performed. In the presence of CN^{-} and Cu^{2+}, the sensor BTZ showed impressive colorimetric changes, going from pale yellow to orange and pale yellow to dark yellow, respectively. In the meantime, FL spectrum (Cu^{2+}) and UV–vis spectroscopy (CN^{-}/Cu^{2+}) were used to assess the sensing features. The plausible binding mechanisms of CN^{-} and Cu^{2+} ions with sensor BTZ have been studied using the ^{1}H NMR titration, Job's plot and DFT technique. The bathochromic shift produced by the intramolecular charge transfer (ICT) transition may have been the source of the phenomenon. Furthermore, CN^{-} ion in the commercial substance is quickly identified and measured with the naked eye by using sensor BTZ. It was found that the BTZ's LOD for CN^{-} and Cu^{2+} was 0.280×10^{-7} M and 1.153×10^{-7} M, respectively. Moreover, 1:1 binding ratio for the reaction of CN^{-} and Cu^{2+} ions with sensor BTZ were demonstrated by Job's plot, which was dependent on analytical data. The findings show that BTZ is an easy-to-use and practical probe for concurrently sensing cyanide and copper ions in environmental samples and living cells that have less cytotoxicity.

1. Introduction

Anions are prevalent in landscape and play roles in industrial, agricultural, and biological processes as well as causes pollution [1]. Detecting anions, especially cyanide, which is a potent poison due to its interference with electron transport through binding to cytochrome *c* oxidase, has gained significant attention. Concurrently, cyanide is necessary for chemical industrial operations like metallurgy, manufacture, polymers, and electroplating [2]. Cyanide's toxicity is well-established, and despite its danger. It is also widely used in various industries, releasing it as a contaminant into the environment. Efficient sensing systems are needed to monitor cyanide concentrations in contamination sources [3,4]. Anions like fluoride, nitrate, and cyanide are recognized pollutants, with cyanide originating from industries like petrochemicals, plating, mining, metal electroplating, and others [5]. It's known for its toxic effects on the body, affecting the central nervous system, blood vessels, and eyes [6–8].

* Corresponding author.
E-mail addresses: skarpagam80@yahoo.com, skarpagam@vit.ac.in (S. Karpagam).

https://doi.org/10.1016/j.heliyon.2024.e38593
Received 30 May 2024; Received in revised form 23 September 2024; Accepted 26 September 2024
Available online 4 October 2024

Due to their important functions and possible toxicity to humans and the environment, heavy and transition metal ions have attracted a lot of research when it comes to chemosensor identification [9,10]. Copper ions are crucial for physiological processes, gene expression, and the human nervous system. Maintaining copper homeostasis is essential for good health, but unregulated Cu(II) intake can lead to neurodegenerative disorders like Alzheimer's, Parkinson's, Menke's, Wilson's, and prion diseases. Conversely, copper deficiency is linked to myelopathy. Moreover, copper is a significant environmental pollutant due to its widespread use in various fields. Even submicromolar concentrations of copper ions can harm microorganisms [11–13]. Consequently, there remains a significant demand for the development of highly sensitive and selective chemosensors for copper. Monitoring various cations in different environments is a challenge for researcher. Copper plays both role, essential for human health and implicated in toxicological issues, holds a prominent place in industrial and biological system [14–16].

Various methods such as Atomic Absorption Spectrometry (AAS) [17], Inductive Coupled Mass Atomic Emission Spectrometry (ICP-AES) [18], and Resonance Rayleigh Scattering (RRS) [19] spectroscopy are commonly used for ion detection. However, these approaches are often complex, expensive, and susceptible to interference from other metal ions. Hence it is necessity to develop a fast, highly sensitive, and selective analytical method. In recent research, chemosensors for both cations and anions have gained attention for their affordability, real-time monitoring, and excellent sensitivity and selectivity [20]. In the case of detecting cyanide and copper ions, the focus has turned towards novel colorimetric sensors that enable easy visual detection of color changes without the need of any costly equipment [21]. Colorimetric materials have several benefits, including excellent selectivity, simplicity, quick response, and low cost [22–25].

Benzothiazoles and quinoline are prominent heterocyclic compounds that are celebrated for their diverse pharmacological activities. They also exhibit outstanding photophysical properties, including high quantum yields, elevated molar extinction coefficients, large Stokes shifts, and excellent photostability. These features have driven researchers to develop fluorescent probes and chemosensors using these compounds. Typically, these sensors combine a benzothiazole or quinoline moiety with a small organic recognition unit attached to the benzothiazole ring. The presence of nitrogen and sulfur atoms within the ring system enhances their coordination ability, making them effective for various sensing applications.

Despite their potential, existing chemosensors based on benzothiazole and quinoline face significant challenges, such as solubility, complex synthesis, interference, slow detection, and high costs, limiting their practical applications. To address these limitations, we have developed a novel Benzothiazole-quinoline based colorimetric sensor (BTZ). This new sensor provides a straightforward and cost-effective method for the selective and sensitive detection of Cu^{2+} and CN^{-} ions through distinct color and spectral responses. The BTZ sensor improves upon previous methods by offering a faster response time, lower detection limits, simplified synthesis, and reduced interference from other transition metal ions. Therefore, there's a need for colorimetric sensors capable of identifying both CN^{-} and Cu^{2+} in aqueous solutions. To address this need, a novel multifunctional chemosensor labelled as BTZ has been developed that can identify CN^{-} and Cu^{2+} based on distinctive color variations over other ions. As part of this effort, a novel asymmetric chemosensor, referred to as BTZ, was designed and synthesized by combining quinoline aldehyde and hydrazine benzothiazole, followed by a condensation reaction with a catalytic amount of sulfuric acid. The resulting sensor, BTZ, can discern CN^{-} through a visible color variation from pale yellow to orange, with high selectivity in a DMF:Water (9:1) mixture. Furthermore, it responds to Cu^{2+} both colorimetrically and fluorescence while unaffected to other metal ions.

A number of colorimetric and fluorometric sensors that use azomethine chromophore have surfaced in recent years to identify harmful ions in a variety of methods [26–29]. In our recent works, cyanide ion was recognized using simple deprotonation mechanism [30,31]. On the other hand, limited has been published regarding the creation of extremely specific sensors for concurrent identification of anions and cations. This has led to the development of a colorimetric sensor based on the azomethine compound with appropriate substituents, that allows for the focused and in tandem detection of Cu^{2+} and CN^{-} in an aqueous DMF solution. Notably, a color shift from pale yellow to dark yellow for Cu^{2+} and from pale yellow to orange for CN^{-} allows visual observation of these sensing processes. The detection threshold of BTZ against CN^{-} and Cu^{2+} was 0.280×10^{-7} M and 1.153×10^{-7} M, respectively. The advancement of efficient sensors may be advanced by the design of chemosensors that respond to copper cations and cyanide anions in two different ways through distinctive mechanisms.

2. Experimental section

2.1. Reagents and solvents

The initial components, including hydrazine benzothiazole and thiazole aldehyde, were procured from suppliers such as Sigma-Aldrich and TCI. Metal salts, encompassing both cations and anions, were obtained from Sd-fine Ltd and employed in their as-received state without additional purification. All solvents underwent a thorough drying and distillation process in accordance with established protocols before their use.

2.2. General structural characterization

NMR spectra were acquired with a Bruker spectrometer operating at 400 MHz, and the chemical shifts were expressed in δ (ppm). KBr discs on a Shimadzu FT-IR spectrometer covering the range of 400–4000 cm^{-1} was used to generate FT-IR spectra. HRMS spectra were captured using a WATER-XEVO G2-XS-QT instrument. Absorption spectra were recorded employing an Agilent 8453 UV–vis spectrophotometer, while diffuse reflectance spectra were collected using a Jasco-v-670 spectrophotometer. Steady-state photoluminescence (PL) measurements were conducted with an Edinburg FLS 980 spectrometer. SEM and EDAX analysis are taken from

CARL ZEISS model, EVO 18 research make.

2.3. Cell culture and cytotoxicity study

For the bio-imaging investigation, RAW264.7 macrophages cells were obtained from NCCS, Pune. These cells were cultured in Dulbecco Modified Eagle's Media supplemented with 10 % Fetal Bovine Serum, and maintained in a 5 % CO_2, 37 °C humidified incubator [32]. In the cytotoxicity assessment, cells were grown until they reached 80 % confluency. Subsequently, the cells were harvested and seeded in a 96-well plate at a density of 1×10^4 cells per well, followed by an overnight incubation. The following day, the cells were subjected to various concentrations of BTZ, ranging from 10 μM to 100 μM, to assess the compound's cytotoxic effects. The cells were then placed in the incubator for 72 h. After the treatment period, 20 μl of MTT solution was added to the cells, which were then incubated for an additional 3 h in the dark. 100 μl DMSO was added to dissolve the crystals and the optical density (OD) was measured at 570 nm using a microplate reader from BioTek, USA, and the percentage of cell viability was calculated.

2.4. Cell bio-imaging study

The cells were grown in a complete medium until they reached confluency. Subsequently, cells were collected and then seeded in six-well plates at a density of 1×10^5 cells in each well. They were left to incubate overnight in a humidified incubator. After 24 h, the cells were subjected to the lowest concentration of BTZ for 1 h. This was followed by exposure to a 0.5 μM concentration of copper for an additional 30 min to facilitate interaction. Once the incubation period was completed, the cells were thoroughly washed with cold 1X PBS three times to eliminate any residues. Finally, images were captured using a fluroscence microscope (EVOS M5000 Imaging System).

2.5. General procedure for UV–vis and FL spectroscopy

2.5.1. Preparation of stock solution

A stock solution of BTZ (3.04 mg in 10 ml) with a concentration of 10^{-3} M was prepared in DMF solvent. From this stock solution, the required dilution was performed to achieve a final concentration of 10^{-5} M. It's worth noting that the initial concentration of each cation and anion stock solution in water was also set at 10^{-3} M. These prepared solutions were subsequently utilized in UV–Visible spectroscopic investigations.

2.5.2. Measurement of UV–vis and FL spectroscopy

A 2 ml quartz cuvette was loaded with a substantial volume of the BTZ solution and metal ion solutions in a 9:1 ratio. UV–Visible spectroscopy was employed to measure the absorbance at the designated working wavelength both prior to and subsequent to the addition of the metal ion solutions. Absorbance spectra for BTZ interacting with various ions were recorded in the wavelength range of 200–800 nm. The same procedure was repeated for fluorescence (FL) spectroscopy.

2.6. Synthesis of 2-(2-(quinolin-3-ylmethylene)hydrazineyl)benzo[d]thiazole, (BTZ)

A simple one step reaction was carried out to synthesis BTZ. Hydrazino benzothiazole (500 mg, 3 mmol) and quinoline-3-aldehyde (476 mg, 3 mmol) were dissolved in 10 ml of ethanol. Further 3 drops of Conc. Sulfuric acid were added to the above mixture and stirred over 3 h at room temperature (Scheme 1). The formed orange precipitate was filtered using Whatman TLC plate, washed thrice with water, and dried. The reaction was monitored through TLC. The product obtained was orange powder. ^{1}H NMR (400 MHz, DMSO-d_6) δ(ppm): 11.57 (S, 1H), 9.32 (S, 1H), 8.63 (S, 1H), 7.12–8.36 (m, 9H). ^{13}C NMR (100 MHz, DMSO-d_6) δ(ppm): 160.93, 159.70, 158.75, 155.25, 130.84, 115.81, 114.50, 123.45, 118.26. FTIR (KBr cm^{-1}): 3270 (-NH frequency), 2934 (-CH frequency), 1660 (-C=N frequency). HRMS *m/z* calculated for $C_{17}H_{12}N_4S$:304.08, found: 305.07.

2.7. Computational studies

Insights into the structural and functional attributes were gained through density functional theory (DFT) calculations. The selection of the DFT functional and the combination of the basis set were crucial in understanding bonding patterns, electronic charge distribution, and molecular orbital energy. Geometries for BTZ, BTZ-CN^-, and BTZ-Cu^{2+} in both gaseous and liquid phases were optimized using the Becke's three-parameter and Lee-Yang-Parr functional (B3LYP) along with the Los Alamos National Laboratory 2-double-z (LANL2DZ) basis set. Specifically, a 6-311G(d,p) basis set was applied for N, O, H, and C atoms, while LANL2DZ was used for

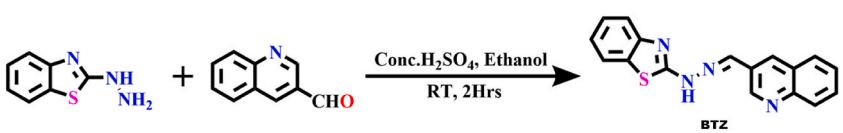

Scheme 1. The synthesis process of BTZ.

the metal complex [33]. Moreover, HOMO-LUMO energy band gap values were determined for BTZ, BTZ-CN^-, and BTZ-Cu^{2+}. Time-dependent density functional theory was employed to analyze UV–Vis absorption spectra for these compounds [34]. The computational investigations were conducted using the G16 package, and electronic geometries and frontier molecular orbital structures were visualized using Gauss View [35].

3. Results and discussion

3.1. Synthesis and characterizations

To prepare the BTZ probe, we initiated the process with hydrazino benzathiazole, synthesized according to the previously reported protocol [36] (Scheme 1). Utilizing a one-step reaction procedure, we synthesized the BTZ probe by combining hydrazino benzothiazole and quinoline-3-aldehyde in a 10 ml ethanol solution with a catalytic amount of concentrated sulfuric acid, characterizing the product through various analytical techniques (Scheme 1). BTZ, being equipped with an –NH functional group, presents a significant possibility of deprotonation when exposed to anions. In the ^{1}H NMR spectrum of BTZ obtained in DMSO-d6, two singlet signals were observed, corresponding to the –NH and -N = CH functional groups, situated at δ 9.35 ppm and 8.63 ppm, respectively, confirming the formation of an imine linkage in the BTZ probe. Additionally, the high-resolution mass spectrum (HRMS) of BTZ displayed the molecular ion peak of (BTZ + H^+) at m/z = 305.0748 (calculated m/z = 304.0783), providing further confirmation of the BTZ probe's formation. Detailed characterization information is provided in the Supplementary Materials accompanying this manuscript (Figs. S1–S2). **3.2. Colorimetric Study**.

3.1.1. Selectivity of *BTZ* towards CN^- and Cu^{2+}

The selectivity of the BTZ probe towards various anions was investigated by introducing different anions, including Br^-, Cl^-, CN^-, CO_3^{2-}, F^-, HSO_4^-, $H_2PO_4^-$, I^-, NO_3^-, NO_2^-, OH^-, PO_4^{3-}, and S^{2-} in DMF-water (9:1) solution (Fig. 1a). Notably, the sensor BTZ exhibited a striking color shift, transitioning from light yellow to orange, specifically when CN^- ions was added, distinguishing it from the other experienced ions. Moreover, the manufactured sensor showed remarkable sensitivity to CN^- ions, exhibiting a quick colorimetric change in a matter of seconds. On addition of copper ion, the color change occur within 10s while cyanide ion is so faster which turns orange color within 5s. Additionally, the introduction of CN^- ions caused a significant red shift from 359 nm to 461 nm (longer wavelength) of 102 nm difference in the UV–Vis spectroscopy of the BTZ sensor, attributed to an enhanced intramolecular charge transfer (ICT). This change in charge transfer formation arises from the robust relationship between CN^- ions and the hydrazine proton of BTZ in aqueous DMF medium, whereas no significant signal changes were induced by other evaluated anions, as illustrated in Fig. 1a.

Furthermore, the BTZ probe demonstrated an instant color shift, transitioning from pale yellow to dark yellow, when exposed to copper ion in aqueous DMF medium at room temperature (Fig. 1b). In contrast, the adding of distinct metal ions, such as Cd^{2+}, Co^{2+}, Cr^{3+}, Cu^{2+}, Eu^{3+}, Fe^{3+}, Hg^{2+}, Mg^{2+}, Mn^{2+}, Ni^{2+}, and Pb^{2+} in the DMF: H2O (9:1) mixture, did not produce significant changes (Fig. 1b). This observed selective color change offers a valuable method for the colorimetric recognition of Cu^{2+} ions. The BTZ probe exhibits a distinct absorbance peak at approximately 359 nm. Upon introducing a copper solution, a sudden peak emerges at around 441 nm, providing conclusive evidence of BTZ's remarkable selectivity for copper ions. The shift from the original peak at 359 nm to the newly observed peak at 441 nm indicates a substantial difference of 82 nm (Fig. 2b). This observation underscores the specific and sensitive response of the BTZ probe to the presence of copper ions.

Color alterations were readily noticeable to the naked eye, and fluorescence quenching was observed under UV light (Fig. S3). This observable color transformation arises from the complexation of the ligand with metal ions [29,30].

3.1.2. Sensitivity of BTZ towards CN^- and Cu^{2+}

Utilizing the absorption spectra, the sensing capabilities of the BTZ sensor were assessed by introducing a standard CN^- solution into BTZ solution (90:10, v/v). After the CN- ions were added, the absorbance at 359 nm gradually decreased and a new absorption band appeared at 461 nm. The absorption spectra titration of BTZ with cyanide ions is shown in Fig. 2c. The conspicuous and

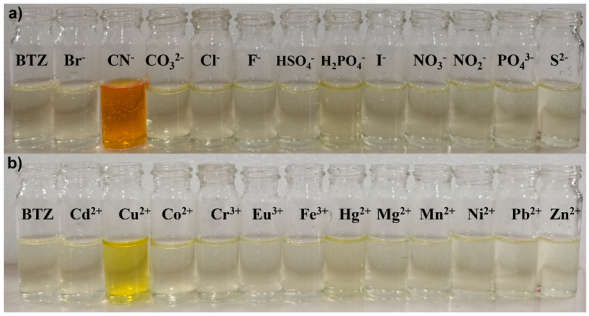

Fig. 1. Naked eye changes of BTZ with a) different anions and b) different cations under normal light.

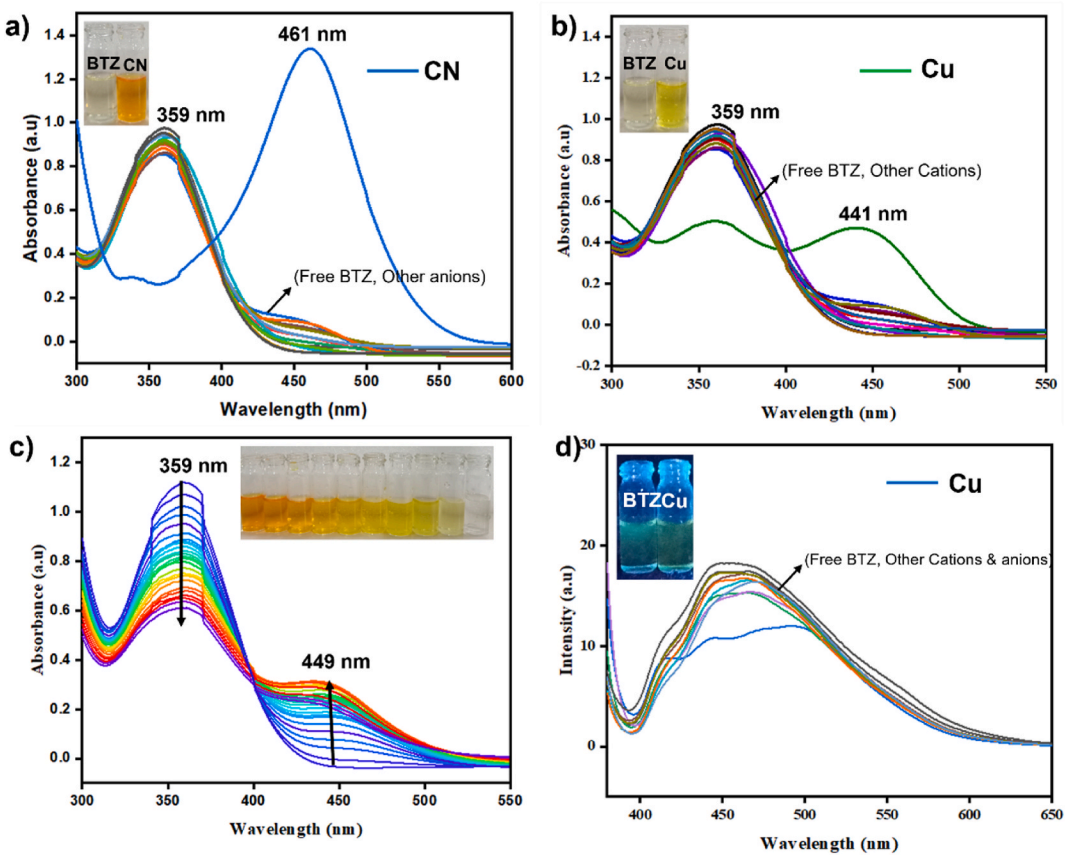

Fig. 2. a) Absorbance spectra of BTZ with various anions in DMF:H_2O (9:1), b) Absorbance spectra of BTZ with various cations in DMF:H_2O (9:1), c) Absorbance spectra titration of BTZ with gradual addition of CN^- ions (2 equivalent). The blue line indicates the initial state of BTZ and the red line indicates the spectra after reaction saturation on addition of Cyanide to BTZ solution, and d) Fluorescence response of BTZ against cations and anions. (For interpretation of the references to color in this figure legend, the reader is referred to the Web version of this article.)

significant absorption red shift of 102 nm in the UV–vis spectroscopy, along with the remarkable color alteration in comparison to BTZ, provides strong evidence that the developed chemosensor BTZ is effective in the analysis of cyanide ions. Furthermore, a well-defined isobestic point at 399 nm was detected, signifying the development of a stable composite among BTZ and cyanide ions.

The determination of the association constant between BTZ and Cu^{2+} metal ions was carried out through a UV–Vis titration of copper ions with the BTZ sensor (Fig. S3c). The consecutive addition of copper ions to the BTZ solution was exactly noted. As copper metal ions were introduced to the BTZ solution, the peak at 442 nm progressively increased, while the peak at 359 nm decreased. This overlapping of absorption peaks led to the appearance of an isosbestic point, signifying the development of a metal complex. Notably, the isosbestic point was also observed at 434 nm in the presence of copper ions.

To elucidate the binding stoichiometry between BTZ and cyanide ions as well as copper ions, Job's plot was employed in this experiment. The results clearly demonstrate that the sensor BTZ forms a 1:1 binding stoichiometry with both cyanide ions and copper ions (refer to Figs. 3c and S3). Furthermore, to evaluate the sensitivity of the BTZ sensor, absorbance responses were plotted against the concentrations of cyanide ions and Cu^{2+}, revealing a linear relationship in two distinct ranges (refer to Fig. 3a and **b**). The detection limit for BTZ in detecting CN^- and Cu^{2+} was calculated using Equation (1).

$$LOD = 3\sigma/m \quad (1)$$

where.

σ - standard deviation
m - slope of the calibration line

Eq. (1), the LOD for sensor BTZ towards CN^- and Cu^{2+} was found to be 28 nM and 1.153×10^{-7} M. Table S1 [37–42] and Table S2 [31,43–47] provide a comparison of recent research studies on chemo-sensors designed for sequential detection of Cu^{2+} and CN^- through complexation and displacement mechanisms. Our system offers several advantages over others, notably a lower limit of detection (LOD)." The binding constant of BTZ- CN^- and BTZ- Cu^{2+} from B-H plot was found to be 1.647×10^5 M^{-1} and 2.995×10^8

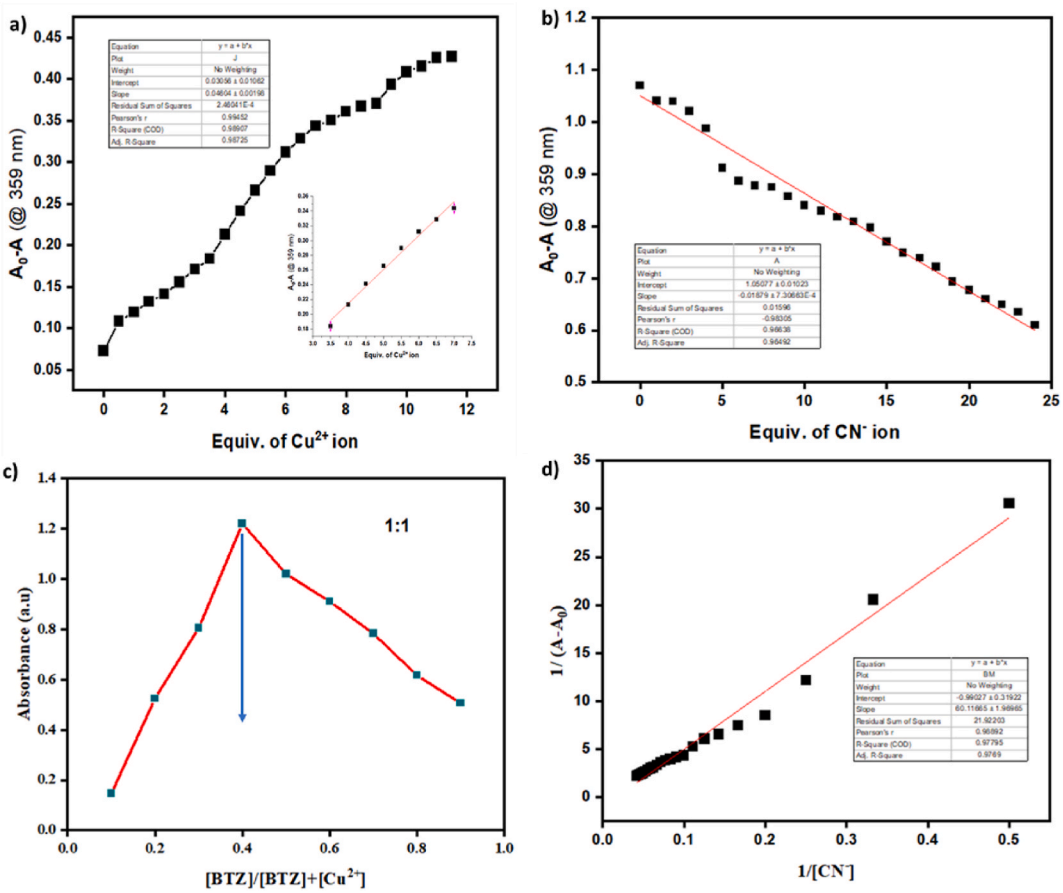

Fig. 3. Absorbance spectra titration of BTZ with gradual addition of a) Cu^{2+} ions, b) CN^{-} ion in DMF:H_2O (9:1), c) Job's plot between BTZ and Cu^{2+}, and c) B-H plot of BTZ-CN^{-} from titration spectrum.

M^{-1}.

3.1.3. Reversibility and interference study

Optical reversibility and reusability are characteristics observed in only a limited number of reported chemosensors. Many well-known cyanide detectors employ irreversible methods, limiting their applicability in various analytical scenarios. To test the reusability of the BTZ sensor, systematic UV repeated titration tests were conducted with BTZ-CN^{-} by adding increasing amounts of trifluoroacetic acid (TFA), as illustrated in Fig. 4b. The absorption spectrum at 359 nm gradually diminished after the addition of approximately 2.0 equiv. of TFA to the complex solution. The sensor's ability to provide a reusable response was demonstrated through consecutive titration cycles, with TFA added after each cycle. Notably, the bare eye color transition from pale yellow to orange and back to pale yellow reoccurred at approximately 60-s intervals.

To unveil the dynamic response of the BTZ-Cu^{2+} interaction, experiments testing the binding reversibility were carried out. The introduction of EDTA into the solution containing the BTZ-Cu^{2+} complex retained the color, shifting from yellow to the pale-yellow characteristic of the BTZ compound. Following this, the addition of a Cu^{2+} ion solution to the same mixture led to the restoration of both color and intensity, thereby confirming the chemical reversibility of the BTZ-Cu^{2+} binding (refer to Fig. 4a). This reversible ability was confirmed through up to three cycles [38], demonstrating the ecological recyclability and reusability of the BTZ compound.

Additionally, we conducted interference study using solutions comprising CN^{-} and various different ions. As illustrated in Fig. 5a, there was no notable alteration in the detection of CN^{-} even in the occurrence of various different anions. Likewise, a similar outcome was detected for the bare eye recognition of Cu^{2+} amidst the presence of various cations and anions that interfere, as depicted in Fig. 5a. Upon the addition of a cyanide ion solution to a solution containing BTZ and copper, a noticeable transformation occurs as the dark yellow hue shifts to a vibrant orange color. This observed color change serves as a visual indicator of the interference and complexation of CN ions in the chemical reaction. The shift in color is indicative of the formation of a distinct molecular complex involving BTZ, Cu^{2+}, and CN^{-} ions. In the examination of the two-step UV–vis study involving the interaction of CN^{-} ion solution with a BTZ-Cu^{2+} solution, the initial stage is characterized as the "complexation approach." This denotes that in the first step, a complex is formed between the BTZ-Cu^{2+} complex and cyanide ions. The subsequent phase is identified as the "displacement approach," indicating that in this step, a displacement reaction occurs, leading to the production of $[Cu(CN)_x]^{n-}$ (shown in Fig. 5). The observed color

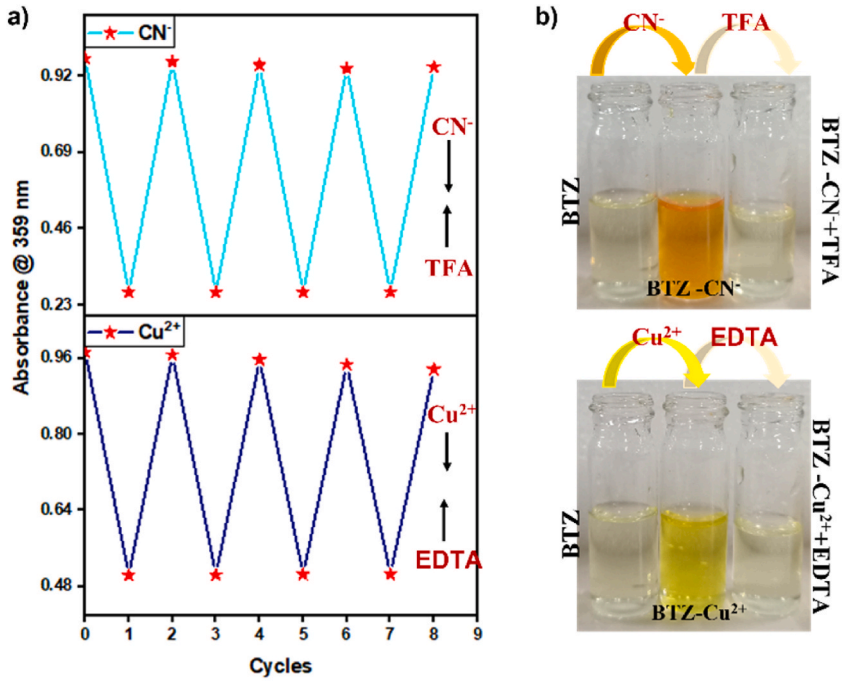

Fig. 4. (a) Change in absorption spectra of BTZ (1×10^{-5}) on the alternative addition of CN^-- TFA and Cu^{2+}- EDTA. The sky-blue color represents the spectrum of reversibility study of BTZ-CN^- and blue line represents the spectrum of reversibility study of BTZ-Cu^{2+}. b) Photographs of BTZ-CN^- before and after addition of TFA and BTZ-Cu^{2+} before and after addition of EDTA. (For interpretation of the references to color in this figure legend, the reader is referred to the Web version of this article.)

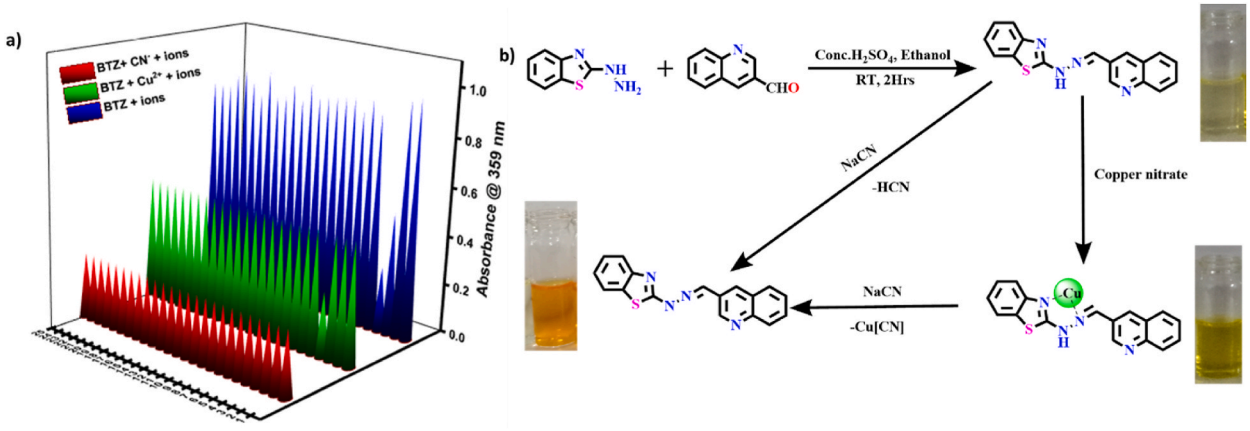

Fig. 5. a) Interference study of BTZ for common ions (anions and cations) in DMF:H_2O. Representation. 1) BTZ, 2) Cd^{2+}, 3) Cu^{2+}, 4) CN^-, 5) Co^{2+}, 6) Cr^{3+}, 7) Eu^{3+}, 8) Fe^{3+}, 9) Hg^{2+},10) Mg^{2+}, 11) Mn^{2+}, 12) Ni^{2+}, 13) Pb^{2+}, 14) Zn^{2+}, 15) Br^-, 16) Cl^-, 17) CO_3^{2-}, 18) F^-, 19) HSO_4^-, 20) $H_2PO_4^-$, 21) I^-, 22) NO_3^-, 23) NO_2^-, 24) PO_4^{3-}, and 25) S^{2-}. b) Expected mechanism of BTZ towards Cu^{2+}, CN^-, and interference effect (reaction) of CN^- ion towards BTZ + Cu^{2+} solution.

change from dark yellow to orange provides visual evidence of these sequential processes, supporting the conclusion that complexation and displacement approaches are integral to the studied reaction. These distinct spectral and colorimetric changes affirm the capability of the BTZ sensor for effective naked-eye detection of CN^- and Cu^{2+} ions, demonstrating remarkable selectivity in aqueous DMF solutions.

Furthermore, we explored the impact of the instantaneous addition of CN^- and Cu^{2+} ions on the UV–Vis spectrum of BTZ (refer to Fig. 3). Upon the simultaneous introduction of Cu^{2+} (1.0 equiv) and CN^- (1.0 equiv), the BTZ solution underwent a noticeable color shift from light yellow to orange. This suggests that, under these conditions, the developed sensor predominantly detected CN^- ions. Intriguingly, even during the titration of BTZ-CN^- with Cu^{2+}, the orange color of the solution remained nearly unchanged, indicating stability in color up to 3 equiv. of Cu^{2+} ions.

3.1.4. Effect of pH for detection of Cu^{2+} and CN^{-}

The impact of pH on the sensing characteristics of BTZ, BTZ-Cu^{2+}, and BTZ-CN^{-} was investigated within the pH range of 3–11. As depicted in Fig. S4, both the yellow color and absorbance intensity of BTZ, in the presence of Cu^{2+}, remained consistent across a broad pH spectrum from 3 to 9, with particular stability observed in acidic solutions. Conversely, in the absence of Cu^{2+}, BTZ exhibited no discernible alterations in color or absorption spectra within the pH range of 3–9. Therefore, BTZ demonstrates high selectivity and sensitivity as a colorimetric chemosensor for Cu^{2+} and CN^{-} within the pH range of 3–9. This makes it well-suited for the recognition of copper ions in diverse ecological and physiological conditions. Hence, the chemosensor BTZ is effective for the detection of Cu^{2+} and CN^{-} over an extensive pH range, particularly in neutral aqueous solutions.

3.1.5. Binding mechanism of BTZ - Cu^{2+} and BTZ - CN^{-}

The stoichiometry ratio of BTZ and cyanide ions, as well as copper ions, was determined using Job's plot, revealing a 1:1 ratio for both interactions. Initial absorbance titration experiments confirmed a 1:1 coordination ratio between BTZ and Cu^{2+}, with noticeable spectral shifts indicating coordination of the benzothiazole nitrogen atom with Cu^{2+}. Subsequent ^{1}H NMR titration in DMSO-d_6 further elucidated the binding sites, showing significant weakening of the -NH proton peak at δ 9.3 ppm and slight downward shifts in aryl proton signals upon addition of Cu^{2+}, affirming the coordination bonds formed as shown in Fig. 6.

Further understanding of the binding mechanisms was gained through theoretical studies employing density functional theory (DFT). The optimized structures and HOMO-LUMO energy levels revealed electron transfer upon complex formation, with a narrower energy gap observed in the BTZ-Cu^{2+} complex compared to free BTZ. This theoretical validation supported the experimental findings, explaining the red-shift in the absorption spectrum upon addition of Cu^{2+} and indicating the increased stability of the BTZ-Cu^{2+} complex.

Moreover, NMR titration experiments were pivotal in elucidating the binding mechanism and detection strategies of BTZ with cyanide ions. Unlike with Cu^{2+}, no discernible alterations in the chemical shift of aromatic protons were observed upon addition of cyanide ions. However, the complete disappearance of the -NH peak at δ 9.3 ppm signified deprotonation, suggesting a chemodosimetric interaction between BTZ and cyanide ions (Fig. 7). This interaction, along with subsequent intra-ligand charge transfer, triggered a shift in color from pale yellow to orange, providing insights into the mechanism of cyanide ion sensing. Additionally, stoichiometric analysis, both experimentally and theoretically, confirmed a 1:1 ratio of BTZ-Cu^{2+} and BTZ-CN^{-}, highlighting the specificity of the interactions and providing valuable insight into the complexation behavior. Additionally, Fig. S5 illustrates that upon titration of the BTZ solution with Cu (II) and CN ions, the resulting BTZ-Cu^{2+} and BTZ-CN^{-} complexes displayed molecular ion peaks at m/z 304.0710 and 367.0083. These peaks correspond to [1BTZ + 1 M + H^{+}], providing clear evidence for the anticipated 1:1 stoichiometric ratio between BTZ and the respective metal ions.

The surface morphology of BTZ, BTZ-CN^{-}, and BTZ-Cu^{2+} complexes was analyzed through SEM imaging, as illustrated in Fig. 8. The BTZ sample exhibited a crystalline and smooth surface with a morphology characterized by cylindrical crystal-like structures. In contrast, both BTZ-CN^{-} and BTZ-Cu^{2+} samples displayed a more clustered, crystal-like morphology. Additionally, energy dispersive X-ray analysis (EDX) was employed to identify the elements present in these samples. The EDX results revealed that BTZ contained carbon, nitrogen, and sulfur, while BTZ-Cu^{2+} contained carbon, nitrogen, sulfur, and copper, indicating the successful formation of a copper complex with the BTZ probe. These findings confirm the complex formation involving the BTZ probe.

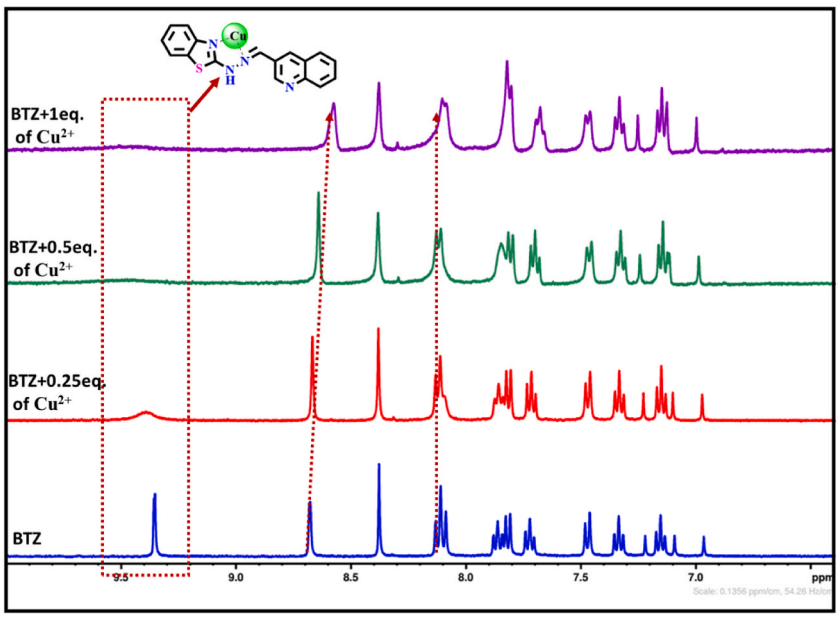

Fig. 6. ^{1} H NMR spectral titration of BTZ with Cu^{2+} ions in DMSO-d_6.

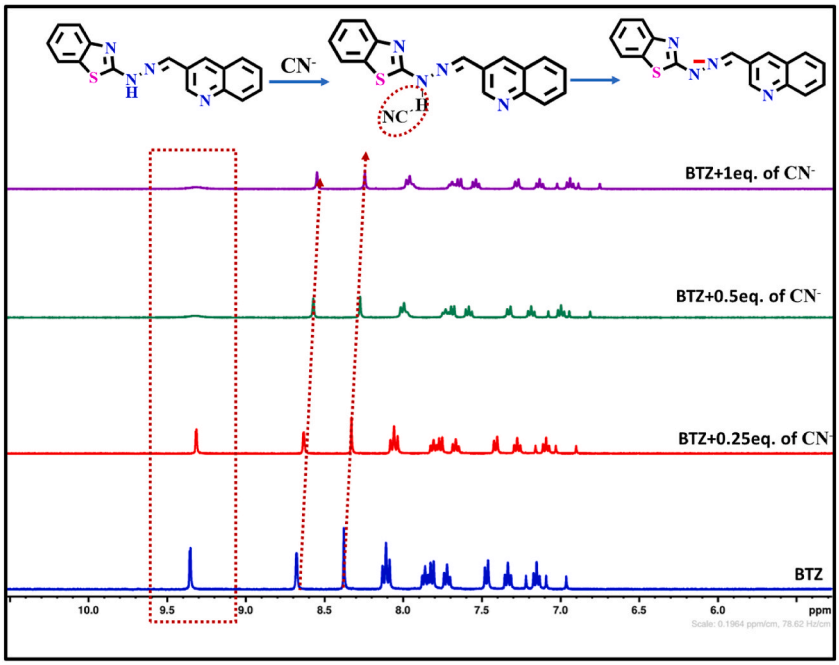

Fig. 7. ^{1}H NMR spectral titration of BTZ with CN^{-} ions in DMSO-d_6 and Proposed response mechanism for the BTZ sensor involving coordination bonds.

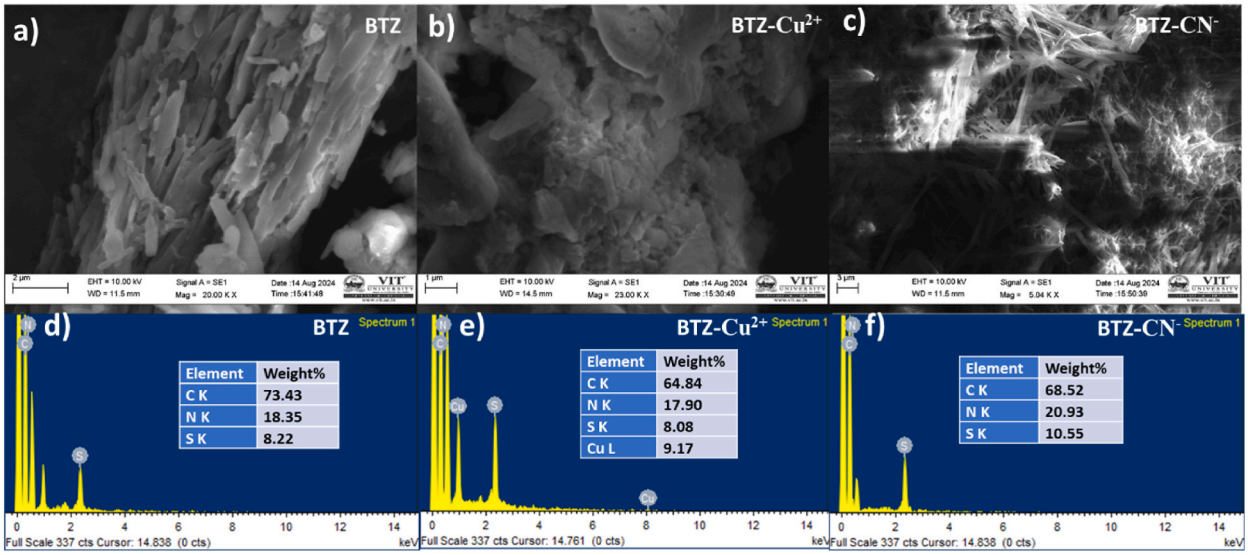

Fig. 8. SEM (a–c) and EDX (d–f) images of BTZ, BTZ-CN^{-}, and BTZ-Cu^{2+}.

3.1.6. Theoretical studies

The structural optimization of BTZ, BTZ-CN^{-}, and BTZ-Cu^{2+} complexes was conducted using density functional theory (DFT) with the B3LYP functional and 6-31+G** basis set for C, H, N, and S atoms, while LANL2DZ basis set was employed for metal complexes. In the pristine BTZ compound, the HOMO electron density was evenly distributed across the entire molecule, with the LUMO primarily localized in the conjugated imine and aromatic quinoline ring. Upon complexation with Cu^{2+}, a noticeable shift in electron density was observed, with the HOMO centered on both the metal ion and the benzothiazole moiety, while the LUMO predominantly resided in the conjugated quinoline and imine as shown in Fig. S6. While, BTZ binding with cyanide ion, the HOMO centered on benzothiazole and partially with quinoline moiety, LUMO predominantly quinoline, N present in BTZ and imine.

The optimization of the BTZ-Cu^{2+} complex revealed bond lengths of CH=N-Cu and C=N-Cu at 1.886 Å and 1.853 Å respectively, indicating enhanced stability in metal-ligand coordination (See Fig. 9). Furthermore, the calculated HOMO-LUMO energy gap was

determined to be 3.98 eV for BTZ, 3.07 eV for BTZ- Cu^{2+} and 1.44 eV for BTZ-CN^-, signifying the extent of electronic transitions within the molecule. Stoichiometric analysis, both theoretically and experimentally, confirmed a 1:1 ratio of BTZ-Cu^{2+} and BTZ-CN^-, providing valuable insight into the complexation behavior (Fig. S6).

Time-dependent DFT (TD-DFT) calculations were then employed to investigate electronic transitions in the absorption spectra. The formation of intraligand charge-transfer bands was observed at 341 nm (BTZ), 437 nm (BTZ + Cu^{2+}), and 561 nm (BTZ + CN^-), with metal complexation inducing significant bathochromic shifts in absorption spectra (shown in Fig. S7). This phenomenon, supported by DFT data, elucidated the colorimetric response to metal ions, showcasing the intricate interplay between electronic structure and complexation dynamics.

3.1.7. Solid medium sensing of Cu^{2+} and CN^-

Solid phase visual detection of metal ion and anion offers convenience, time efficiency, and cost-effectiveness for on-site monitoring of toxic substances [48,49]. TLC plate were used to evaluate the chemosensor BTZ's suitability for use on-site. First, 100 μM solution of BTZ in DMF was applied on thin strips of TLC plate, which were then allowed to air dry before being sliced into tiny round pieces. The TLC plate exhibited a slight yellow color under normal light in the solid phase. Subsequently, different anions and metal ions (10 μL) in water were drop-cast onto the TLC plate pre-coated with BTZ, revealing a significant color change yellow for Cu^{2+} and orange for CN^- in the solid-state. Moreover, the selectivity of BTZ towards Cu^{2+} was confirmed by the absence of color change upon addition of aqueous solutions containing various metal ions and anions, ensuring the TLC plate exclusively detect Cu^{2+} and CN^- (Fig. 10). This direct detection capability of BTZ on a solid phase highlights its potential for on-site monitoring of Cu^{2+} levels in environmental samples, demonstrating superior sensitivity, detection limit, and synthetic ease.

The ability of BTZ to detect analytes directly on a solid phase coupled with its selectivity and sensitivity. This shows that the chemosensor BTZ is a promising tool for various on-site monitoring applications. Through meticulous experimentation utilizing silica gel-coated TLC plate, BTZ demonstrated robust performance in detecting Cu^{2+} and CN^- ions, showcasing its utility for environmental sample analysis. The distinct color changes observed in the presence of target analytes underscore BTZ's effectiveness and potential as a cost-effective solution for rapid and reliable on-site detection needs, emphasizing its advantages over conventional methods.

4. Biological applications

4.1. Cell viability and toxicity

The suitability of the chemosensor BTZ for biological imaging was assessed by evaluating its cytotoxicity using trypan blue and hemocytometer technique. Across a range of concentrations (10–100 μM), BTZ demonstrated negligible toxicity towards RAW macrophage cell lines, as evidenced by the maintenance of cell viability above 90 % (Fig. S8). These results confirm the safety of BTZ for cellular applications, indicating its potential for bioimaging studies. Notably, even at the highest tested concentration, BTZ did not induce any adverse effects on cell viability, further underscoring its biocompatibility. Therefore, the decision was made to proceed with the lowest concentrations of BTZ, supplemented with 0.5 μM of Cu^{2+} ion. For subsequent bioimaging experiments, it is necessary to ensure minimal impact on cell health while enabling effective metal ion sensing.

The evaluation of BTZ's cytotoxicity highlights its promise as a viable option for biological imaging applications. By demonstrating negligible toxicity towards RAW macrophage cell lines across a range of concentrations, BTZ emerges as a safe and reliable tool for studying cellular processes. The ability to maintain high cell viability, even at the highest concentration tested, underscores the biocompatibility of BTZ and its potential for use in sensitive cellular assays. Moreover, the inclusion of 0.5 μM of Cu^{2+} ion alongside the lowest concentrations of BTZ further enhances its utility for metal ion sensing in bioimaging studies, offering researchers a versatile and non-toxic approach for visualizing biological processes at the cellular level.

4.2. Bio-imaging study

In fluorescence imaging study, RAW macrophages cell lines were treated with the lowest concentration of BTZ (10 μM) along with Cu^{2+} ion concentrations of 0.5 μM, followed by a 0.5-h incubation period. The fluorescence imaging investigation revealed detectable peaks in the green channel upon treatment with the receptor compounds. However, upon addition of Cu^{2+} ion, there was a significant decrease in fluorescence intensity observed in Fig. 11, suggesting an interaction between the BTZ probe and copper within the cellular environment, resulting in a decrease at the subcellular level. The fluroscence images of BTZ probes demonstrated predominant

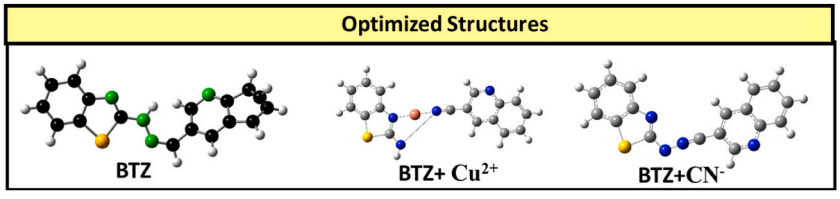

Fig. 9. Optimized structures (BTZ, BTZ + Cu^{2+}, BTZ + CN^-) with B3LYP/LanL2DZ level of theory via the Gaussian 09 package and their energy gap Contour plots.

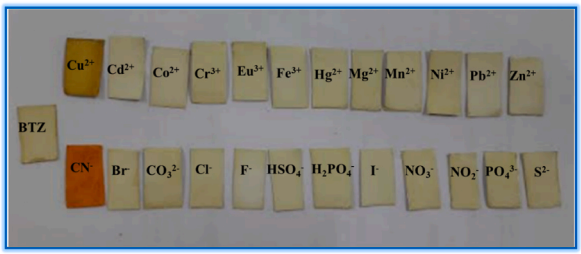

Fig. 10. Solid state naked eye detection of copper and cyanide against different metal ions and anions by chemosensor BTZ. (pale yellow color- BTZ + different metal ions/anions, yellow color- BTZ + Cu^{2+}, orange color- BTZ + CN^{-}). (For interpretation of the references to color in this figure legend, the reader is referred to the Web version of this article.)

fluorescence distribution within the cytoplasm, indicating intracellular accumulation.

In Fig. 11, cells exhibited fluorescence signal in the green channel post-incubation with the chemosensor BTZ (10 μM), indicating effective entry of the chemosensor BTZ into the live RAW macrophages cell lines. Subsequently, the fluorescence signal in the green channel weakened upon addition of copper ions in RAW macrophages cell lines treated with BTZ. These imaging results collectively demonstrate the ability of the chemosensor BTZ to detect copper ions in RAW macrophages cell lines.

4.3. Water sample application

The chemosensor BTZ was used to detect Cu^{2+} and CN^{-} ions in water samples from places around Vellore, Tamilnadu. Different types of water like tap water, river water, and ground water were tested. BTZ was tested with varying concentrations of spiked cyanide water solution, and the changes were observed using UV–Vis spectroscopy. The results showed that BTZ could detect Cu^{2+} and CN^{-} ions with a high recovery rate (95–98 %) and low variation between measurements (RSD values). This demonstrates that BTZ is effective in sensing these ions in different water samples. (Table S3). The statistical data were confirmed and quantified using water samples through ICP-MS. The results indicated that the proposed BTZ sensor material shows promise for real-time environmental sensing applications, offering a cost-effective solution without sacrificing ion-sensing performance.

5. Conclusion

In conclusion, the BTZ sensor exhibits remarkable selectivity and sensitivity for CN^{-} and Cu^{2+} ions in aqueous DMF solutions. The distinct colorimetric responses shifting from light yellow to orange with CN^{-} and from pale yellow to yellow with Cu^{2+} ion. It also showed a significant red shift in the UV–Vis spectra, highlight its robust detection capabilities. The fluorescence sensing of Cu^{2+} ion demonstrates intra-ligand charge transfer, and 1:1 binding stoichiometry coupled with low detection limits confirms its high sensitivity and precision. The sensor's optical reversibility, resistance to interference, and stability across a wide pH range add to its practical utility. Insights from NMR titrations and theoretical studies elucidate the coordination bonds between BTZ and metal ions, supporting its effectiveness in qualitative copper ion assessment. Its low cytotoxicity and potential for cellular uptake make it a promising candidate for biological sensing applications. Future work should focus on exploring the sensor's interactions with a broader range of metal ions, assessing its performance in real-world contexts, and investigating opportunities for functionalization to enhance its applicability across various sensing scenarios.

Data availability

Data included in article/supp. material/referenced in article.

CRediT authorship contribution statement

P.S. Umabharathi: Writing – original draft, Methodology, Investigation. **S. Karpagam:** Writing – review & editing, Supervision, Project administration, Conceptualization. **Tiasha Dasgupta:** Validation, Software, Investigation. **Ramasamy Tamizhselvi:** Visualization, Software, Investigation.

Declaration of competing interest

The authors declare the following financial interests/personal relationships which may be considered as potential competing interests:S. Karpagam reports financial support and administrative support were provided by Vellore Institute of Technology.

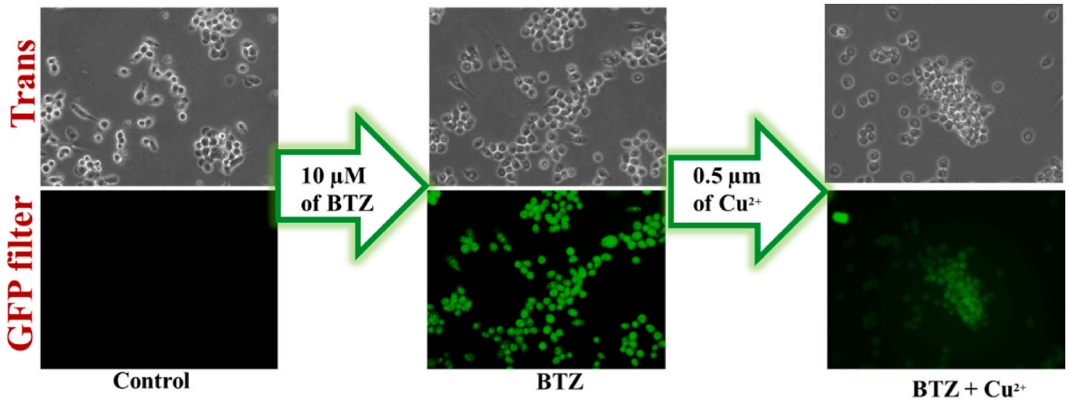

Fig. 11. Intercellular imaging of BTZ with Cu^{2+} ion visualized under confocal laser scanning microscope.

Acknowledgement

The authors greatefully acknowledge VIT University for providing VIT seed grant contributed only for consumables and instrumental facilities

Appendix A. Supplementary data

Supplementary data to this article can be found online at https://doi.org/10.1016/j.heliyon.2024.e38593.

References

[1] K. Goria, A. Bharti, S. Raina, R. Kothari, V. V Tyagi, H.M. Singh, G. Kour, Low-cost adsorbent biomaterials for the remediation of inorganic and organic pollutants from industrial wastewater: eco-friendly approach, in: Sustain. Mater. Sens. Remediat. Noxious Pollut., Elsevier, 2022, pp. 87–112.
[2] A. Moaddeli, M. Fereidooni, M. Nabipour, R. Parchami, M. Tabrizchi, Cyanide determination in postmortem blood samples using Headspace-Ion Mobility Spectrometry (HS-IMS), Forensic Chem 37 (2024) 100539.
[3] J. Graham, J. Traylor, Cyanide Toxicity, 2018.
[4] H.B. Leavesley, L. Li, K. Prabhakaran, J.L. Borowitz, G.E. Isom, Interaction of cyanide and nitric oxide with cytochrome c oxidase: implications for acute cyanide toxicity, Toxicol. Sci. 101 (2008) 101–111.
[5] S.R. Mousavi, M. Balali-Mood, B. Riahi-Zanjani, M. Sadeghi, Determination of cyanide and nitrate concentrations in drinking, irrigation, and wastewaters, J. Res. Med. Sci. Off. J. Isfahan Univ. Med. Sci. 18 (2013) 65.
[6] S.M. MacKenzie, Complex Hydrocarbons in the Saturn System, University of Idaho, 2017.
[7] A. Dasgupta, A. Wahed, Clinical Chemistry, Immunology and Laboratory Quality Control: a Comprehensive Review for Board Preparation, Certification and Clinical Practice, 2013.
[8] A. Dasgupta, A. Wahed, A. Dasgupta, A. Wahed, Common poisonings including heavy metal poisoning, Clin. Chem. Immunol. Lab. Qual. Control. (2014) 337–351.
[9] D. Ayodhya, Recent progress on detection of bivalent, trivalent, and hexavalent toxic heavy metal ions in water using metallic nanoparticles: a review, Results, Chem 5 (2023) 100874.
[10] L.A. Malik, A. Bashir, A. Qureashi, A.H. Pandith, Detection and removal of heavy metal ions: a review, Environ. Chem. Lett. 17 (2019) 1495–1521.
[11] E. V Stelmashook, N.K. Isaev, E.E. Genrikhs, G.A. Amelkina, L.G. Khaspekov, V.G. Skrebitsky, S.N. Illarioshkin, Role of zinc and copper ions in the pathogenetic mechanisms of Alzheimer's and Parkinson's diseases, Biochem. 79 (2014) 391–396.
[12] Y.H. Hung, A.I. Bush, R.A. Cherny, Copper in the brain and Alzheimer's disease, JBIC, J. Biol. Inorg. Chem. 15 (2010) 61–76.
[13] L. Chen, J. Min, F. Wang, Copper homeostasis and cuproptosis in health and disease, Signal Transduct. Target. Ther. 7 (2022) 378.
[14] Z. Gerdan, Y. Saylan, A. Denizli, Recent advances of optical sensors for copper ion detection, Micromachines 13 (2022) 1298.
[15] T. Chopra, S. Sasan, L. Devi, R. Parkesh, K.K. Kapoor, A comprehensive review on recent advances in copper sensors, Coord. Chem. Rev. 470 (2022) 214704.
[16] S. Sharma, K.S. Ghosh, Recent advances (2017–20) in the detection of copper ion by using fluorescence sensors working through transfer of photo-induced electron (PET), excited-state intramolecular proton (ESIPT) and Förster resonance energy (FRET), Spectrochim. Acta Part A Mol. Biomol. Spectrosc. 254 (2021) 119610.
[17] S. Sharma, J. Singh, N. Singh, G. Hundal, Spectroscopic and theoretical evaluation of solvent-assisted, cyanide selectivity of chromogenic sensors grounded on mesitylene platform and their biological applications, Sensors Actuators, B Chem. 225 (2016) 141–150, https://doi.org/10.1016/j.snb.2015.11.026.
[18] E. Webb, D. Amarasiriwardena, S. Tauch, E.F. Green, J. Jones, A.H. Goodman, Inductively coupled plasma-mass (ICP-MS) and atomic emission spectrometry (ICP-AES): versatile analytical techniques to identify the archived elemental information in human teeth, Microchem. J. 81 (2005) 201–208.
[19] M. Chen, H.-H. Cai, F. Yang, D. Lin, P.-H. Yang, J. Cai, Highly sensitive detection of chromium (III) ions by resonance Rayleigh scattering enhanced by gold nanoparticles, Spectrochim. Acta Part A Mol. Biomol. Spectrosc. 118 (2014) 776–781.
[20] T. Simon, M. Shellaiah, V. Srinivasadesikan, C.-C. Lin, F.-H. Ko, K.W. Sun, M.-C. Lin, Novel anthracene-and pyridine-containing Schiff base probe for selective "off–on" fluorescent determination of Cu 2+ ions towards live cell application, New J. Chem. 40 (2016) 6101–6108.
[21] J. Isaad, A. El Achari, A novel sugar pyrazolin-5-one based optical chemosensor for sequential detection of copper (II) and cyanide ions in real samples. Experimental and theoretical studies, J. Mol. Struct. 1228 (2021) 129771.
[22] G. Fukuhara, Analytical supramolecular chemistry: colorimetric and fluorimetric chemosensors, J. Photochem. Photobiol. C Photochem. Rev. 42 (2020) 100340.

[23] D.A. McNaughton, M. Fares, G. Picci, P.A. Gale, C. Caltagirone, Advances in fluorescent and colorimetric sensors for anionic species, Coord. Chem. Rev. 427 (2021) 213573.
[24] P.R. Dongare, A.H. Gore, Recent advances in colorimetric and fluorescent chemosensors for ionic species: design, principle and optical signalling mechanism, ChemistrySelect 6 (2021) 5657–5669.
[25] Z. Aydin, M. Keles, Colorimetric detection of copper (II) ions using schiff-base derivatives, ChemistrySelect 5 (2020) 7375–7381.
[26] X. Zhang, L.-Y. Shen, Q.-L. Zhang, X.-J. Yang, Y.-L. Huang, C. Redshaw, H. Xu, A simple turn-off Schiff base fluorescent sensor for copper (II) ion and its application in water analysis, Molecules 26 (2021) 1233.
[27] R. Khalid, S.A. Shahzad, M.A. Assiri, T. Javid, H. Irshad, M.Z. Ullah, AIE active fluorescent probe for the detection of cyanide ion through fluorescence enhancement in real samples: an integrated extensive fluorescence and DFT studies, Microchem. J. 200 (2024) 110264.
[28] J. Isaad, F. Malek, A. El Achari, Colorimetric and fluorescent probe based on coumarin/thiophene derivative for sequential detection of mercury (II) and cyanide ions in an aqueous medium, J. Mol. Struct. 1270 (2022) 133838.
[29] V. Venkatesan, R. Selva Kumar, S.K. Ashok Kumar, S.K. Sahoo, Visible colorimetric sensing of Zn2+ and CN− by diaminomaleonitrile derived Schiff's base and its applications to pharmaceutical and food sample analysis, Inorg. Chem. Commun. 130 (2021), https://doi.org/10.1016/j.inoche.2021.108708.
[30] P. Purushothaman, P.S. Umabharathi, S.G. Sureanthiran, V. Harish, S. Karpagam, Short communication A potent ratiometric detection and estimation of cyanide in the mainstream smoke of tobacco products by spectroscopic technique, Inorg. Chem. Commun. 158 (2023) 111564, https://doi.org/10.1016/j.inoche.2023.111564.
[31] P.S. Umabharathi, P. Purushothaman, S. Karpagam, T. Dasgupta, R. Tamizhselvi, A one-pot synthesized chemodosimetric chemosensor for highly sensitive cyanide ion detection in aqueous Media and from tobacco smoke, ChemistrySelect 9 (2024) e202303893.
[32] A.H. Fronk, E. Vargis, Methods for culturing retinal pigment epithelial cells: a review of current protocols and future recommendations, J. Tissue Eng. 7 (2016) 2041731416650838.
[33] R.M.M. Sumpter, Theoretical Studies of the Ground and Low-Lying Excited States of [3, 3'] Bidiazirinylidene (C2N4), Tetramethyleneethane Diradical, and Arsenic and Selenium Oxides, The University of North Dakota, 2012.
[34] P. Boulet, H. Chermette, C. Daul, F. Gilardoni, F. Rogemond, J. Weber, G. Zuber, Absorption spectra of several metal complexes revisited by the time-dependent density-functional theory-response theory formalism, J. Phys. Chem. A. 105 (2001) 885–894.
[35] M. Frisch, G.W. Trucks, Hb Schlegel, G.E. Scuseria, M.A. Robb, J.R. Cheeseman, J.A. Montgomery Jr., T. Vreven, K.N. Kudin, Jc Burant, Gaussian 03, Revision C. 02, Gaussian, Inc., Wallingford, CT, 2004, p. 4.
[36] R. Yadav, D. Meena, K. Singh, R. Tyagi, Y. Yadav, R. Sagar, Recent advances in the synthesis of new benzothiazole based anti-tubercular compounds, RSC Adv. 13 (2023) 21890–21925.
[37] D. Maity, V. Kumar, T. Govindaraju, Reactive probes for ratiometric detection of Co2+ and Cu + based on excited-state intramolecular proton transfer mechanism, Org. Lett. 14 (2012) 6008–6011, https://doi.org/10.1021/ol302904c.
[38] J. Nootem, R. Daengngern, C. Sattayanon, W. Wattanathana, S. Wannapaiboon, P. Rashatasakhon, K. Chansaenpak, The synergy of CHEF and ICT toward fluorescence 'turn-on' probes based on push-pull benzothiazoles for selective detection of Cu2+ in acetonitrile/water mixture, J. Photochem. Photobiol. Chem. 415 (2021), https://doi.org/10.1016/j.jphotochem.2021.113318.
[39] K. Wang, W. Feng, Y. Wang, D. Cao, R. Guan, X. Yu, Q. Wu, A coumarin derivative with benzothiazole Schiff's base structure as chemosensor for cyanide and copper ions, Inorg. Chem. Commun. 71 (2016) 102–104, https://doi.org/10.1016/j.inoche.2016.07.013.
[40] P. Purushothaman, S. Karpagam, Thiophene-appended benzothiazole compounds for ratiometric detection of copper and cadmium ions with comparative density functional theory studies and their application in real-time samples, ACS Omega 7 (2022) 41361–41369.
[41] P. Piyanuch, S. Wangngae, A. Kamkaew, W. Wattanathana, S. Wannapaiboon, S. Impeng, W. Maneeprakorn, V. Promarak, K. Chansaenpak, Ultrasensitive fluorogenic chemosensor based on ESIPT phenomenon for selective determination of Cu2+ ion in aqueous system and its application in environmental samples and biological imaging, Dye. Pigment. 205 (2022) 110532, https://doi.org/10.1016/j.dyepig.2022.110532.
[42] L.G. Teixeira Alves Duarte, F.L. Coelho, J.C. Germino, G. Gamino da Costa, J.F. Berbigier, F.S. Rodembusch, T.D. Zambon Atvars, A selective proton transfer optical sensor for copper II based on chelation enhancement quenching effect (CHEQ), Dye. Pigment. 181 (2020) 1–7, https://doi.org/10.1016/j.dyepig.2020.108566.
[43] Z.M. Dong, W. Wang, Y. Bin Wang, J.N. Wang, L.Y. Qin, Y. Wang, A reversible colorimetric chemosensor for "Naked Eye" sensing of cyanide ion in semi-aqueous solution, Inorganica Chim. Acta. 461 (2017) 8–14.
[44] R.S. Fernandes, N. Dey, Acyl hydrazone-based reversible optical switch for reporting of cyanide ion in industrial wastewater samples, J. Mol. Struct. 1262 (2022), https://doi.org/10.1016/j.molstruc.2022.132968.
[45] S. Dey, C. Sen, C. Sinha, Chromogenic hydrazide Schiff base reagent: spectrophotometric determination of CN− ion, Spectrochim. Acta Part A Mol. Biomol. Spectrosc. 225 (2020), https://doi.org/10.1016/j.saa.2019.117471.
[46] A. Roniboss, R. Nishanth Rao, K. Chanda, M.M. Balamurali, Hydrazide derived colorimetric sensor for selective detection of cyanide ions, Inorg. Chem. Commun. 134 (2021), https://doi.org/10.1016/j.inoche.2021.108965.
[47] P. Purushothaman, P.S. Umabharathi, S.G. Sureanthiran, V. Harish, S. Karpagam, A potent ratiometric detection and estimation of cyanide in the mainstream smoke of tobacco products by spectroscopic technique, Inorg. Chem. Commun. 158 (2023) 111564.
[48] A. Ranolia, P. Rani, G. Joshi, R. Kumar, S. Kumar, P. Kumar, S. Singh, J. Sindhu, Precisely designed NIR based conjugated framework as a solid state emitter for selective recognition of cyanide ion in solid state and cancer cells, J. Photochem. Photobiol. Chem. 449 (2024) 115373.
[49] A. Maji, K. Aich, A. Biswas, S. Gharami, B. Bera, T.K. Mondal, Efficient solid-and solution-state emissive reusable solvatochromic fluorophores for colorimetric and fluorometric detection of CN, Analyst. 149 (2024) 1557–1570.